Real-Time Dynamic Model Learning and Adaptation for Underwater Vehicles

Joshua D. Weiss
Mechanical and Aerospace Engineering Department
Naval Postgraduate School
Monterey, CA

Noel E. Du Toit
Mechanical and Aerospace Engineering Department
Naval Postgraduate School
Monterey, CA

***Abstract*— Precision control of Unmanned Underwater Vehicles (UUVs) requires accurate knowledge of the dynamic characteristics of the vehicles. However, developing such models are time and resource intensive. The problem is further exacerbated by the sensitivity of the dynamic model to vehicle configuration. This is particularly true for hovering-class UUVs since sensor payloads are often mounted outside the vehicle body. This paper presents a method to learn a dynamic model for such a hovering-class UUV in real time from motion and position measurements. System identification techniques are employed to estimate equations of motion coefficients. Initial results on the approach are presented.**

Keywords—Unmanned Underwater Vehicle; System Identification; Hydrodynamic Model; Online Model Learning; Autonomous Underwater System

I. Introduction

The Center for Autonomous Vehicle Research (CAVR) at the Naval Postgraduate School is developing a robotic diver assistant to share the work and operating space with human divers. This assistant can improve the safety, efficiency, and effectiveness of dive operations in all domains of professional diving, from police to science divers. Of particular interest in this research is the potential benefit to the Salvage, Explosive Ordinance Disposal (EOD), and Undersea Rescue operations of the Department of the Navy. The application requires operation of a hovering-class UUV (see Fig. 1) in close proximity to humans as well as other features (e.g., structures, the sea bottom, etc.), which in turn requires precision control on the vehicle. The application will require testing of a vehicle in multiple configurations (i.e., different payload combinations) as well as the development of various perception and control strategies. As a result, an effective and efficient manner of developing a dynamic model will greatly assist in executing the robotic diver assistant program.

The goal of this research is to learn a parameterized dynamic model for an UUV in real time, and to automate the procedure where possible. Each change in payload configuration changes the weight distribution, center of buoyancy, and drag properties of the platform (i.e., changes the dynamics), requiring a new model. This work will ultimately produce a hydrodynamic model of the SeaBotix vLBV300 Remotely Operated Vehicle (ROV), the development platform for the CAVR robotic diver assistant.

A hydrodynamic model of a UUV can be developed from first principles. Fossen [1] presents a detailed approach exploring the kinematics and dynamics that make up a complete model for a generic six degree of freedom vehicle. This generic model is specialized for the development platform to account for the unique design, relatively slow speeds of operation, and high level of maneuverability. The resulting model is then utilized to investigate online model parameter learning.

Online model learning, also known as system identification, attempts to learn model parameters by commanding specific vehicle movements [2-4]. System identification techniques are distinguished by when they are applied to gathered data and what type of model is of interest. One approach is to capture the vehicle motion for a commanded behavior and then to choose parameters that best represent all the data offline (i.e., regression techniques, such as Linear Least Squares Regression [8]). Alternatively, model parameters can be estimated online: the estimate is continually updated as new data becomes available. It is often possible to adapt offline techniques for online implementation (e.g., Least Squares Regression), or to develop new techniques entirely (e.g., Gradient Descent methods). These techniques can be applied to either parametric- or so-called non-parametric models. Parametric models are informed by the physical characteristics of the system derived from first principles (e.g., the generic hydrodynamic model developed by Fossen [1]). Non-parametric models, such as Neural Networks [10], use non-physical basis functions to capture input-output and as a result the resulting parameters lack physical interpretation. The same parameter identification techniques can be applied to either type of model. An important consideration in system identification is parameter convergence to the true value. This problem is well-studied (e.g., [2]) and requires "Persistence of Excitation" (i.e., the excitation signal must be sufficiently rich to excite relevant modes).

System identification has been applied to various UUVs. Doherty [6] and Prestero [7] employed empirical techniques to estimate specific parameters of the REMUS Autonomous Underwater Vehicle (AUV). Chen, et al. [5] used a projective mapping method to estimate the dynamic parameters of a hovering class UUV similar to the work presented here. Alternatively, methods have been investigated to measure hydrodynamic coefficients directly (e.g., using free decay pendulum motion [9]. In this work, an external motion capture system is used to track the development vehicle and to learn the model parameters online.

In this work, a propulsion model is developed (Section II) and the general hydrodynamic model presented by Fossen [1] is specialized for the development platform, the SeaBotix vLBV300 (Section III). System Identification techniques are presented in Section IV and specialized for the vLBV300 in Section V. Convergence is verified for a known system in simulation before the techniques are applied to the vLBV300 in Section VI. Concluding remarks are included in Section VI.

II. SEABOTIX VLBV300 MINIROV

A. General Characteristics

The vLBV300, manufactured by SeaBotix, Inc. of San Diego, California, is a miniROV remotely operated vehicle. It is operated through a tether and can be controlled by multiple user interfaces including a joystick or a computer program via a high-level, 4-DOF interface (surge, sway, heave, yaw) or a low-level, individual-thruster command interface, which results in a 5-DOF system (additionally, roll can be controlled). Data and power are transmitted through the tethered interface. Thus the platform can be leveraged as a Tethered, Hovering-class Autonomous Underwater System (THAUS). For propulsion and maneuvering the vLBV300 uses 6 brushless DC thrusters, four of which are vectored in the horizontal plane (surge, sway, yaw), the angles of which can be manually adjusted, while the remaining two are fixed in the vertical plane (heave, roll). The vehicle can be equipped with a variety of sensors including a controllable HD camera, rear and side cameras, sonars, as well as a grabber arm for in-water intervention. A typical configuration is shown in Figure 1. As configured for this research, the vehicle weighs 20.9 kg in air; is 0.625 m long, 0.39 m wide, and 0.39 m tall; and does not have any ancillary equipment attached besides a BlueView sonar. The aft pair of horizontal thrusters are vectored to an angle of 45 degrees from centerline while the forward pair of horizontal thrusters was vectored to 35 degrees from centerline (see Figure 2). The vertical thrusters are angled at 18 degrees (seer Figure 4) A right handed, body-fixed frame is used with x pointing forward, y pointing right, and z pointing down (see Figure (4)).

Fig. 1. SeaBotix vLBV300 miniROV platform (www.seabotix.com) has been modified to allow tethered, autnonomous operations.

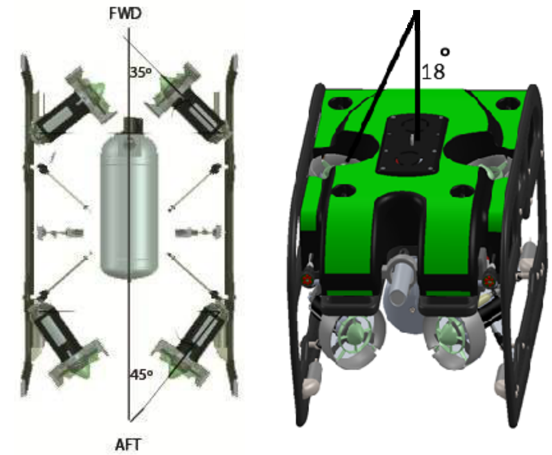

Fig. 2. Horizontal and vertical thruster configuration of the vLBV300

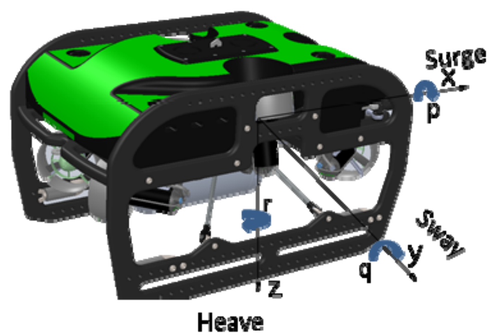

Fig. 3. Diagram showing the right-handed reference frame used in this research.

B. Propulsion Model

Each thruster on the vehicle can be commanded individually, using low-level PWM commands (which are related to RPM). These commands range from -102 to 102. For the aft thruster-pair, the positive direction is defined as producing clockwise rotation of the propeller, which results in motion in the positive (ahead) surge direction. For the forward thrusters, a positive command results in counter-clockwise rotation and therefore also thrust in the positive surge direction. A positive sway command results in the leading edge propellers (right hand set for motion to the right) spinning in the positive direction while the trailing set spins in the negative direction. A positive command to the vertical thrusters results in clockwise rotation and motion in the positive heave (downward) direction. Using these definitions and the thruster geometry the vehicle's propulsion forces are defined. For ease of notation the thrust generated by the horizontal, forward, starboard propeller is referred to here as *FS*. The horizontal, forward, port propeller thrust is referred to as *FP*. The horizontal, aft, starboard propeller thrust is referred to as *AS* and the horizontal, aft, port propeller thrust is referred to as *AP*. The thrust generated by the vertical starboard and vertical port propellers are referred to as *VS* and *VP*, respectively.

$$X_{prop} = \left(AP * c\,\alpha_r - FP * c\,\alpha_f \right) + \left(AS * c\,\alpha_r - FS * c\,\alpha_f \right) \tag{1}$$

$$\begin{aligned} Y_{prop} = &\left(FS * s\,\alpha_f + AS * s\,\alpha_r \right) - \\ &\left(FP * s\,\alpha_f + AP * s\,\alpha_r \right) \\ &-(VL - VR) * s\,\beta \end{aligned} \tag{2}$$

$$Z_{prop} = \left(VL + VR \right) * c\,\beta \tag{3}$$

$$K_{prop} = \left(VL + VR \right) * s\,\beta * LV \tag{4}$$

$$M_{prop} = 0 \tag{5}$$

$$\begin{aligned} N_{prop} = &\left(AP * c\,\alpha_r - FP * c\,\alpha_f \right) * LH_1 + \\ &\left(AS * c\,\alpha_r - FS * c\,\alpha_f \right) * LH_1 + \\ &\left(AP * s\,\alpha_r - FP * s\,\alpha_f \right) * LH_2 + \\ &\left(AS * s\,\alpha_r - FS * s\,\alpha_f \right) * LH_2 + \end{aligned} \tag{6}$$

Note: For ease of notation s● = sin(●), c●=cos(●), and t●=tan(●). *LV, LH_1*, an *LH_2* are moment arms. *LV* is defined as the distance between the centroid of the two vertical propellers while *LH_1* is the distance between the centroid of the propellers of the aft or forward pair, and *LH_2* is defined as the distance between the centroid of the propellers of the right or left side pair. *M_{prop}* is zero in all cases since pitch cannot be controlled on any vehicle considered in this research.

The relationship between low-level PWM commands and a measured force for individual thrusters was determined through in-tank testing using the aft thruster pair only and a Futek USB210 strain gage. The experimentally obtained data is given in Fig. 4 through which a second-order polynomial is fitted:

$$Thrust = 0.006736 PWM^2 - 0.03366 PWM + 0.0684 \tag{7}$$

The results for both the positive and negative direction are virtually identical for commands from 10 to 60, as would be expected from the performance of a fixed pitch propeller. Due to a limitation with the experimental setup, surface effects affected results above a PWM command of 60 (i.e., the 60-102 range). Since the planned vehicle operations will be at low thrust (and speed), this thruster model is sufficient. The results of the regression are compared with the experimental data in Fig. 4.

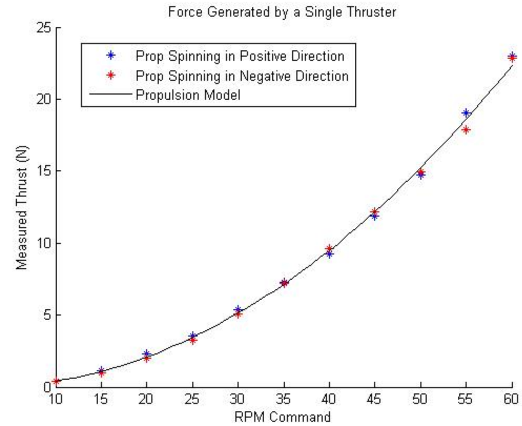

Fig. 4. Propulsion model for a single thruster on the vLBV300 compared with experimental data.

III. Generic Motion Model

A. Full Equations of Motion

The non-linear dynamic equations of motion for a six degree of freedom (DOF) body are presented by Fossen [1] as

$$M\dot{\upsilon} + C(\upsilon)\upsilon + D(\upsilon)\upsilon + g(\eta) = \tau \tag{8}$$

The vector υ contains the body velocities and angular rates,

$$\upsilon = [u, v, w, p, q, r]^T \tag{9}$$

where u is velocity in the surge direction, v is velocity in the sway direction, w is velocity in the heave direction, p is the angular rate about the x-axis of the body frame, q is the angular rate about the y-axis of the body frame, and r is the angular rate about the z-axis of the body.

The vehicle's pose is described by the vector η:

$$\eta = [x, y, z, \phi, \theta, \psi]^T \tag{10}$$

where x, y, and z are the vehicle's position with respect to an inertial reference frame, and ϕ , θ, ψ are Euler angles determined using the zyx-convention.

Vehicle pose dynamics are related to body velocities, angular rates, and the pose itself, by

$$\dot{\eta} = J(\eta)\upsilon \tag{11}$$

$$J = \begin{bmatrix} J_1 & 0_{3\times3} \\ 0_{3\times3} & J_2 \end{bmatrix} \tag{12}$$

where

$$J_1 = \begin{bmatrix} c\psi\, c\theta & -s\psi\, c\phi + c\psi\, s\theta\, s\phi & s\psi\, s\phi + c\psi\, c\phi\, s\theta \\ s\psi\, c\theta & c\psi\, c\phi + s\phi\, s\theta\, s\psi & -c\psi\, s\phi + s\theta\, s\psi\, c\phi \\ -s\theta & c\theta\, s\phi & c\theta\, c\phi \end{bmatrix} \tag{13}$$

$$J_2 = \begin{bmatrix} 1 & s\theta t\theta & c\phi t\theta \\ 0 & c\phi & -s\phi \\ 0 & s\phi / c\theta & c\phi / c\theta \end{bmatrix}. \tag{14}$$

M is the inertia matrix which is the sum of the rigid body mass, M_{RB} , and the added inertia matrix, M_A,

$$M \triangleq M_{RB} + M_A \tag{15}$$

$C(\upsilon)$ is the matrix of Coriolis and centripetal terms and is also the sum of a rigid body, C_{RB}, and added mass, C_A, components:

$$C(\upsilon) \triangleq C_{PB}(\upsilon) + C_A(\upsilon) \tag{16}$$

$D(\upsilon)$ is the damping matrix which is the sum of radiation-induced potential damping due to forced body oscillation, D_P, linear skin friction due to laminar boundary flow and quadratic skin friction due to turbulent flow, D_S, wave drift damping, D_W, and damping due to vortex shedding, D_M,

$$D(\upsilon) \triangleq D_P(\upsilon) + D_S(\upsilon) + D_W(\upsilon) + D_M(\upsilon) \tag{17}$$

g(η) is the vector of gravitational forces and moments,

$$g(\eta) = \begin{bmatrix} (W-B)\mathrm{s}\theta \\ -(W-B)\mathrm{c}\theta\mathrm{s}\phi \\ -(W-B)\mathrm{c}\theta\mathrm{c}\phi \\ -(y_G W - y_B B)\mathrm{c}\theta\mathrm{c}\phi + (z_G W - z_B B)\mathrm{c}\theta\mathrm{s}\phi \\ (z_G W - z_B B)\mathrm{s}\theta + (x_G W - x_B B)\mathrm{c}\theta\mathrm{c}\phi \\ -(x_G W - x_B B)\mathrm{c}\theta\mathrm{s}\phi - (y_G W - y_B B)\mathrm{s}\theta \end{bmatrix} \tag{18}$$

where W is the weight (in air) of the vehicle, $W= mg$, B is buoyant force produced by the fully submerged vehicle, and x_g, y_g, and z_g are the Cartesian coordinates in the body frame of the vehicle's center of gravity while x_b, y_b, and z_b are the Cartesian coordinates in the body frame of the vehicle's center of buoyancy. τ is a vector of the forces and moments exerted on the vehicle by the thrusters. X_{prop} is a force in the surge direction, Y_{prop} is a force in the sway direction; Z_{prop} is a force in the heave direction; K_{prop} is a force in the roll direction; M_{prop} is a force in the pitch direction; and N_{prop} is a force in the yaw direction.

$$\tau = \left[X_{prop}, Y_{prop}, Z_{prop}, K_{prop}, M_{prop}, N_{prop} \right] \tag{19}$$

B. Assumptions and Simplified Equations

In order to model the non-linear dynamics of the UUV, (8) and (11) must be solved for υ and η. Several assumptions are made about the characteristics of the UUV to simplify the components of (8). The vehicle is assumed to be neutrally buoyant ($B=W$) and the tether is assumed to have no effect on vehicle motion or trim. The x and y coordinates of the center of gravity and center of buoyancy are assumed to coincide. Also, since the specific mass distribution of the vehicle is not known, a uniform distribution of mass is assumed [5,6] and the components of the inertia tensor that are off the main diagonal are neglected. The moments of inertia were estimated using the equation for moment of inertia of a square and are I_X= 0.559 kgm^2, I_Y = 0.953 kgm2, and I_Z = 0.90 kgm^2. These assumptions yield:

$$g(\eta) = \begin{bmatrix} 0 \\ 0 \\ 0 \\ -B(z_G - z_B)\mathrm{c}\theta\mathrm{s}\phi \\ B(z_G - z_B)\mathrm{s}\theta \\ 0 \end{bmatrix} \tag{20}$$

$$F_{BK} = B(z_G - z_B)\mathrm{c}\theta\mathrm{s}\phi \tag{21}$$

$$F_{BM} = B(z_G - z_B)\mathrm{s}\theta \tag{22}$$

$$M_{RB} = \begin{bmatrix} m & 0 & 0 & 0 & mz_G & 0 \\ 0 & m & 0 & -mz_G & 0 & 0 \\ 0 & 0 & m & 0 & 0 & 0 \\ 0 & -mz_G & 0 & I_X & 0 & 0 \\ mz_G & 0 & 0 & 0 & I_Y & 0 \\ 0 & 0 & 0 & 0 & 0 & I_Z \end{bmatrix} \tag{23}$$

$$C_{rb}(\upsilon) = \begin{bmatrix} 0_{3\times3} & C_1 \\ C_2 & C_3 \end{bmatrix} \tag{24}$$

where

$$C_1 = \begin{bmatrix} mz_G r & mw & -mv \\ -mw & mz_G r & mu) \\ -m(z_G p - v) & -m(z_G q + u) & 0 \end{bmatrix} \tag{25}$$

$$C_2 = \begin{bmatrix} -mz_G r & mw & m(z_G p - v) \\ -mw & -mz_G r & m(z_G q + u) \\ mv & -mu & 0 \end{bmatrix} \tag{26}$$

$$C_3 = \begin{bmatrix} 0 & I_Z r & -I_Y q \\ -I_Z r & 0 & I_X p \\ I_Y q & -I_X p & 0 \end{bmatrix} \tag{27}$$

Furthermore, the vehicle is assumed to have three planes of symmetry, will be fully submerged for all motion, and will only move at low speeds. Therefore, as per [1] (see equations (2.129) and (2.13)) the following simplified terms are obtained:

$$M_A = -\mathrm{diag}\left(\left[X_{\dot{u}}, Y_{\dot{v}}, Z_{\dot{w}}, K_{\dot{p}} M_{\dot{q}}, N_{\dot{r}} \right]\right) \tag{28}$$

$$C_A(\upsilon) = -\begin{bmatrix} 0 & 0 & 0 & 0 & -Z_{\dot{w}}w & Y_{\dot{v}}v \\ 0 & 0 & 0 & Z_{\dot{w}}w & 0 & -X_{\dot{u}}u \\ 0 & 0 & 0 & -Y_{\dot{v}}v & X_{\dot{u}}u & 0 \\ 0 & -Z_{\dot{w}}w & Y_{\dot{v}}v & 0 & -N_{\dot{r}}r & M_{\dot{q}}q \\ Z_{\dot{w}}w & 0 & -X_{\dot{u}}u & N_{\dot{r}}r & 0 & -K_{\dot{p}}p \\ -Y_{\dot{v}}v & X_{\dot{u}}u & 0 & -M_{\dot{q}}q & K_{\dot{p}}p & 0 \end{bmatrix} \tag{29}$$

Assuming in addition that the vehicle is performing only uncoupled motion with complete turbulent flow, the damping term is in the form:

$$D(\upsilon) = -\text{diag}\left(\left[X_{u|u|}|u|, Y_{v|v|}|v|, Z_{w|w|}|w|, K_{p|p|}|p|, M_{q|q|}|q|, N_{r|r|}|r|\right]\right) \tag{30}$$

Combining all assumptions yields the following simplified dynamic equations for non-coupled motion for the THAUS UUV:

$$\begin{aligned}
X &= (m - X_{\dot u})\dot u - (m - Y_{\dot v})vr + (m - Z_{\dot w})wq - X_{u|u|}u|u| \\
Y &= (m - Y_{\dot v})\dot v - (m - Z_{\dot w})wp + (m - X_{\dot u})ur - Y_{v|v|}v|v| \\
Z &= (m - Z_{\dot w})\dot w - (m - X_{\dot u})uq + (m - Y_{\dot v})vp - Z_{w|w|}w|v| \\
K &= (I_X - K_{\dot p})\dot p + (Y_{\dot v} - Z_{\dot w})wv + (I_Z - I_Y - N_{\dot r} + M_{\dot q})rq \\
&\quad - K_{p|p|}p|p| - F_{BK} \\
M &= (I_Y - M_{\dot q})\dot q + (Z_{\dot w} - X_{\dot u})uw + (I_X - I_Z + N_{\dot r} - K_{\dot p})rp \\
&\quad - M_{q|q|}q|q| + F_{BM} \\
N &= (I_Z - N_{\dot r})\dot r + (X_{\dot u} - Y_{\dot v})uv + (I_Y - I_X + K_{\dot p} - M_{\dot q})rp \\
&\quad - N_{r|r|}r|r|
\end{aligned} \tag{31}$$

IV. System Identification

A. Parameter Estimation for a Static System

Consider a regression model of the form [8]

$$y_i = \varphi_i^1\theta^1 + \varphi_i^2\theta^2 + \ldots + \varphi_i^m\theta^m = \varphi_i^T\theta \tag{32}$$

where y_i, $i=1,2,\ldots,n$, is a series of observations, $\varphi_i = \begin{bmatrix}\varphi_i^1 & \varphi_i^2 & \ldots & \varphi_i^m\end{bmatrix}^T$ are the known regressor functions (which are functions of the states and controls), and $\Theta = \begin{bmatrix}\theta^1 & \theta^2 & \ldots & \theta^m\end{bmatrix}^T$ are the unknown parameters (to be estimated). The goal of online system identification is to recursively estimate the unknown parameters Θ according to some adaptation law as new information becomes available.

Several methods of parameter estimation are available to perform the necessary recursive estimation, including the Gradient Estimator and the Recursive Least Squares (RLLS) estimator. Since the hydrodynamic coefficients are time-invariant and a certain amount of measurement and process noise is expected, the RLLS method was chosen and further investigated. The goal then becomes to minimize the square of the error between the measured and modeled response with respect to Θ as in [2] and [8].

$$\min_{\Theta} V(\Theta, n) = \min_{\Theta} \frac{1}{2}\sum_{i=1}^{n}(y_i - \varphi_i^T\Theta)^2 \tag{33}$$

To accomplish this, let $Y = \begin{bmatrix}y_1 & y_2 & \ldots & y_n\end{bmatrix}^T$ be the set of measurements and define the error terms $\varepsilon_i = y_i - \varphi_i^T\hat\Theta$, where $\hat\Theta$ is the estimated parameter. This can be written in vector notation: $E = \begin{bmatrix}\varepsilon_1 & \varepsilon_2 & \ldots & \varepsilon_n\end{bmatrix}^T$. Finally, let

$$\Phi = \begin{bmatrix}\varphi_1^T \\ \vdots \\ \varphi_n^T\end{bmatrix}$$

then the loss function in eq. (33) can be written as:

$$V(\theta, n) = \frac{1}{2}\sum_{i=1}^{n}\varepsilon_i^2 = \frac{1}{2}E^T E = \frac{1}{2}\|E\|^2 \tag{34}$$

where $E = Y - \Phi\Theta$. This loss function is minimized by:

$$\hat\Theta^* = \left(\Phi^T\Phi\right)^{-1}\Phi^T Y. \tag{35}$$

which requires that $\Phi^T\Phi$ is non-singular.

The recursive form of a least squares estimator is defined by

$$\hat\Theta_i = \hat\Theta_{i-1} + K_i(y_i - \varphi_i^T\hat\Theta_{i-1}) \tag{36}$$

where the filter gain is given by:

$$K_i = P_{i-1}\varphi_i\left(I + \varphi_i^T P_{i-1}\varphi_i\right)^{-1} \tag{37}$$

with $P_i = (I - K_i\varphi_i^T)P_{i-1}$.

B. Parameter Estimation of a Dynamic System

When identifying parameters for a dynamic system, some additional steps are required to write the system in the form of eq. 32. Consider the dynamic system:

$$\begin{aligned}\dot x &= f_0(x,u) + f(x,u) \\ \mathrm{y} &= Cx\end{aligned} \tag{38}$$

where $f_0(x,u)$ represents the known (nominal) dynamics of the system and $f(x,u)$ is the unknown dynamics (to be estimated). Assume $f(x,u)$ has the general form:

$$f(x,u) = \Phi(x,u)\Theta \tag{39}$$

where Θ is the matrix of unknown parameters and $\Phi(x,u)$ is a *known regressor* that consists of known basis functions. If a dynamic model for the system can be derived from first principals (e.g., as in [1]), then this model can be used to define Θ and $\Phi(x,u)$ in order to learn a parametric model. This dynamic model must be converted to a static system in order to apply the system identification techniques of the previous section. This can be accomplished through the introduction of filtered signals. First, rewrite eq. 38 as:

$$\dot x + ax = ax + f_0(x,u) + \Phi(x,u)\Theta \tag{40}$$

A filtered version of x, x_f, is also introduced as

$$\dot x_f + ax_f = ax \tag{41}$$

where a is the filtering time constant. Next, define $z = x - x_f$, then $\dot{z} = \dot{x} - \dot{x}_f$, allowing eq. 40 to be rewritten as:

$$\dot{z} + az = f_0(x,u) + \Phi(x,u)\Theta \tag{42}$$

The right hand terms can be thought of as forcing functions, and the first order ordinary differential equation has the known, unique solution:

$$\begin{aligned} z &= e^{-at}z(0) + \int_0^t e^{-a(t-\tau)} f_0(x,u)d\tau \\ &+ \int_0^t e^{-a(t-\tau)}\Phi(x,u)d\tau\Theta \end{aligned} \tag{43}$$

Assume the initial conditions $x(0)=x_f(0)$ so that $z(0)=0$. Then eq. 43 can be simplified to

$$z(t) = \Phi_0 + \Phi_f\Theta \tag{44}$$

where $\Phi_0 = \int_0^t e^{-a(t-\tau)} f_0(x,u)d\tau$ is the filtered version of $f_0(x,u)$ and $\Phi_f \triangleq \int_0^t e^{-a(t-\tau)}\Phi(x,u)d\tau$ is the filtered version of $\Phi_f(x,u)$. Furthermore, rewriting the measurement equation in terms of z and x_f, the dynamic system is converted into a static system:

$$y - Cx_f - C\Phi_0 = C\Phi_f\Theta \tag{45}$$

Since Φ_0 and Φ_f are filtered states, they can be calculated recursively as:

$$\begin{aligned} \dot{\Phi}_0 &= -a\Phi_0 + f_0(x,u) \\ \dot{\Phi}_f &= -a\Phi_f + f(x,u) \end{aligned} \tag{46}$$

V. System Identification Applied to vLBV300

By exciting specific modes for the vLBV300, individual parameters can be estimated. For example, by commanding thrust in the surge direction only through X_{prop}, only motion in the surge direction is induced, reducing eq. (29) to:

$$\begin{aligned} \dot{u} &= \frac{X_{u|u|}u|u| + X_{prop}}{m - X_{\dot{u}}} \\ \dot{v} &= 0, \dot{w} = 0, \dot{p} = 0, \dot{q} = 0, \dot{r} = 0 \end{aligned} \tag{47}$$

which can be rearranged in regressor-parameter form of eq. (38) as:

$$\dot{u} = \begin{bmatrix} u|u| & X_{prop} \end{bmatrix} \begin{bmatrix} \dfrac{X_{u|u|}}{m - X_{\dot{u}}} \\ \dfrac{1}{m - X_{\dot{u}}} \end{bmatrix} \tag{48}$$

The filtering technique of the previous section can then be applied to this simplified system to obtain a static system and to perform the system identification.

Since the SeaBotix ROV is also controllable in sway, heave, roll and yaw, the following simplifications are similarly possible and the system identification of the previous section can similarly be applied.

Sway:

$$\begin{aligned} \dot{v} &= \frac{Y_{v|v|}v|v| + Y_{prop}}{m - Y_{\dot{v}}} \\ \dot{u} &= 0, \dot{w} = 0, \dot{p} = 0, \dot{q} = 0, \dot{r} = 0 \end{aligned} \tag{49}$$

Heave:

$$\begin{aligned} \dot{w} &= \frac{Z_{w|w|}w|w| + Z_{prop}}{m - Z_{\dot{w}}} \\ \dot{u} &= 0, \dot{v} = 0, \dot{p} = 0, \dot{q} = 0, \dot{r} = 0 \end{aligned} \tag{50}$$

Roll:

$$\begin{aligned} \dot{p} &= \frac{K_{p|p|}p|p| + F_{BK} + K_{prop}}{I_X - K_{\dot{p}}} \\ \dot{u} &= 0, \dot{v} = 0, \dot{w} = 0, \dot{q} = 0, \dot{r} = 0 \end{aligned} \tag{51}$$

Yaw:

$$\begin{aligned} \dot{r} &= \frac{N_{r|r|}r|r| + N_{prop}}{I_Z - N_{\dot{r}}} \\ \dot{u} &= 0, \dot{v} = 0, \dot{w} = 0, \dot{p} = 0, \dot{q} = 0 \end{aligned} \tag{52}$$

However, control in the pitch degree of freedom is not possible (M_{prop}=0), but this mode can be excited by commanding a combination of other modes. An examination of the dynamic equation associated with pitch reveals that by exciting the vehicle in the surge and heave degrees of freedom, the pitch portion of eq. (31) can be excited, resulting in the simplified to $\dot{v} = 0, \dot{p} = 0, \dot{r} = 0$ and:

$$\begin{aligned} \dot{u} &= \frac{-(m - Z_{\dot{w}})wq + X_{u|u|}u|u| + X_{prop}}{m - X_{\dot{u}}} \\ \dot{w} &= \frac{(m - X_{\dot{u}})uq + Z_{w|w|}w|w| + Z_{prop}}{m - Z_{\dot{w}}} \\ \dot{q} &= \frac{-(Z_{\dot{w}} - X_{\dot{u}})uw + M_{q|q|}q|q| + F_{BM}}{(I_Y - M_{\dot{q}})} \end{aligned} \tag{53}$$

The system can be written in the form of eq. (38) as follows:

$$\begin{bmatrix} \dot{u} \\ \dot{w} \\ \dot{q} \end{bmatrix} = f_0\left(u, w, q, X_{prop}, Y_{prop}\right) + \Phi(u, w, q)\Theta \tag{54}$$

where:

$$f_0 = \begin{bmatrix} \dfrac{-(m - Z_{\dot{w}})wq + X_{u|u|}u|u| + X_{prop}}{m - X_{\dot{u}}} \\ \dfrac{(m - X_{\dot{u}})uq + Z_{w|w|}w|w| + Z_{prop}}{m - Z_{\dot{w}}} \\ 0 \\ \end{bmatrix} \quad (55)$$

$$\Phi = \begin{bmatrix} 0 & 0 \\ 0 & 0 \\ q|q| & F_{BM} - (Z_{\dot{w}} - X_{\dot{u}})uw \end{bmatrix} \quad (56)$$

$$\Theta = \begin{bmatrix} \dfrac{M_{q|q|}}{(I_Y - M_{\dot{q}})} & \dfrac{1}{(I_Y - M_{\dot{q}})} \end{bmatrix} \quad (57)$$

It is important to note that the inertia parameters are not identified specifically since they do not appear in the dynamic equations without their corresponding Added Mass term (e.g., I_x and $K_{\dot{p}}$ always appear together). This does not affect the applicability of the mode.

In an effort to verify the system identification approach and investigate Persistence of Excitation for the system, a simulator was developed according to the dynamics presented in Eqs. (29). Chen et al. [5] presents a model for the Seamor hovering-class ROV (the parameters were estimated using the Projective Mapping Method, while the mass and inertia parameters are listed as: mass = 20.4 kg, I_x = 0.429 kgm^2, and $I_y = I_z$ = 0.609 kgm^2). The system identification techniques were in turn applied to the simulated system to verify that the true parameters were estimated. As an example, results of the RLLS surge testing are presented in Fig. 5.

As discussed in [8], Persistence of Excitation is a construct for guaranteeing speed of convergence of the solution to the RLLS problem. Through the verification process of the model it was determined that a sinusoidal input is a sufficient input signal to guaranteed rapid convergence to the true values, but a ramp or a "stair-step" series of ramp inputs are more suitable if, as in this case, testing space and time are limited (due to the test tank facility). The coefficients shown in Figure 6, which was driven by a sinusoidal input, can be seen to rapidly converge to the true, identical values. These results were typical for the other coefficients with the exception of roll. This is due to un-modeled dynamics represented by F_{BM} in equation (51). Chen et al [5] did not present the value for z_B, the position of the center of buoyancy. Without knowing this value, assumed to be zero in the simulation, exact results cannot be achieved. The contribution of z_B to F_{BK} is small due to small induced pitch angles and as such was overcome by the filter with an input signal of very high Persistence of Excitation. Full results are presented in Table I.

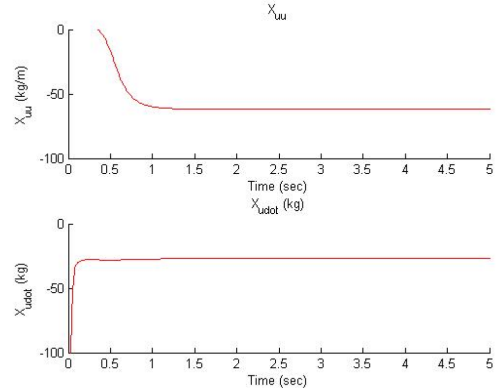

Fig. 5. Convergence of simulator surge parameters

TABLE I. COMPARISON OF FORCE HYDRODYNAMIC PARAMETERS

	True value	Est. value	Units
$X_{\dot{u}}$	-27.08	-27.08	kg
$X_{u\|u\|}$	-61.117	-61.117	kg/m^2
$Y_{\dot{v}}$	-25.952	-25.952	kg
$Y_{v\|v\|}$	-139.81	-139.81	kg/m^2
$Z_{\dot{w}}$	-68.576	-68.576	kg
$Z_{w\|w\|}$	-51.724	-51.724	kg/m^2
$K_{\dot{p}}$	-61.683	-61.683	kgm$^{2/}$/rad
$K_{p\|p\|}$	-12.0	-12.0	kgm$^{2/}$/rad^2
$M_{\dot{q}}$	-79.411	-82.363	kgm$^{2/}$/rad
$M_{q\|q\|}$	-56.61	-58.77	kgm$^{2/}$/rad^2
$N_{\dot{r}}$	-0.154	-0.154	kgm$^{2/}$/rad
$N_{r\|r\|}$	-1.772	-1.772	kgm$^{2/}$/rad^2

VI. EXPERIMENTAL RESULTS

A. Vicon Motion Capture System

Since the vLBV300 is not yet equipped with an onboard Inertial Navigation System (INS), an external motion capture system (VICON) is used to measure the vehicle position and orientation. From these pose measurements, the linear and angular velocities are estimated. The VICON system consists of Infrared LED arrays and cameras that track reflective markers in the operating space. Due to the absorption of electromagnetic signals in water, the current system is only applicable for in-air operation. To overcome this limitation, the vLBV300 has been extended above the water surface with a light-weight, low inertia structure. By tracking this structure and performing the appropriate coordinate transformations, the submerged vehicle's motion can be tracked. This structure will have a small effect on the dynamics of the vehicle, and a more appropriate solution is being investigated (such as relying on INS data instead). The VICON system provides high-accuracy data (<1cm) at high data rates (100 Hz).

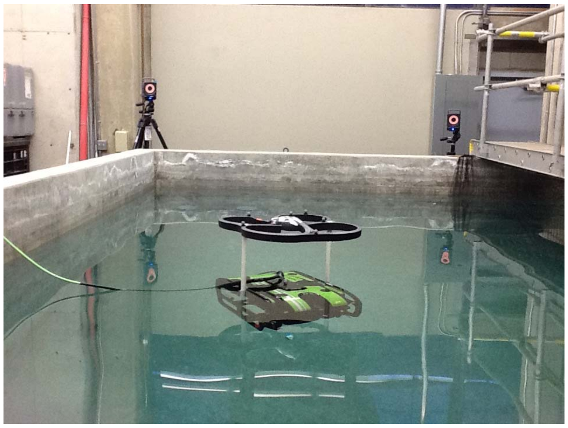

Fig. 6. SeaBotix vLBV300 in the instrumented NPS dive tank

B. SeaBotix Hydrodynamic Testing Results

The vehicle can be commanded accurately through the developed computer interface in the surge, sway, heave, roll, and yaw degrees of freedom in turn by means of a single, constant, low-level PWM command to the appropriate thrusters. It is assumed that the thruster dynamics are significantly faster than the vehicle response so that the commanded PWM control input is best approximated as an instantaneous input. Acceleration greatly affects the assumptions of Section III.B, particularly relating to added mass, and as a result a "stair-step" input, or a series of slightly increasing step commands that allow time for the vehicle to reach steady state, is used to minimize acceleration. Since a RLLS filter's results are only accurate around the trim point, to develop a dynamic model with as wide as range of applicability as possible, coefficients for a low-speed and high-speed trim point must be obtained for as accurate as possible a model to be created. However, because of the limited space available in the NPS tank, high speed operations of sufficient duration to obtain good results are not possible. Only low speed results are presented here.

Body velocities u, v, and w and angular rates p, q, and r are estimated by filtering the high-frequency signal content and taking the time-derivative of the position and orientation provided by the VICON system. The noise inherent to the VICON system is amplified by the time-derivative, which resulted in a noisy input to the RLLS estimator. As a result, estimate convergence was slower, with average convergence time ~5 seconds. The estimation process is further complicated by jumps in pose data (due to marker occlusion), which resulted in spikes in velocity estimates. For example, the convergence of surge-related parameters is presented in Fig. 7.

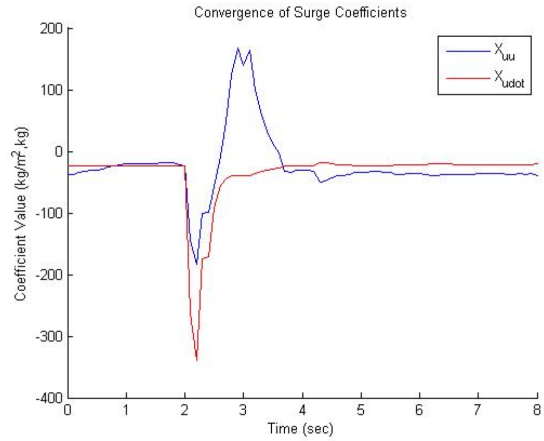

Fig. 7. Convergence of surge coefficients

This convergence is typical for sway, heave, and yaw. The roll and pitch coefficients were not determined to limitations with the experimental setup and will be addressed in future work. The system identification results are presented in Table II (the units are the same as for Table I).

TABLE II. EXPERIMENTALLY DERIVED SEABOTIX HYDRODYNAMIC COEFFICIENTS FOR SURGE, SWAY, HEAVE, AND YAW

$X_{\dot{u}}$	-19.519	$Z_{\dot{w}}$	-21.3776
$X_{u\|u\|}$	-41.343	$Z_{w\|w\|}$	-61.8358
$Y_{\dot{v}}$	17.0621	$N_{\dot{r}}$	-0.9061
$Y_{v\|v\|}$	-7.334	$N_{r\|r\|}$	-0.3491

C. Model Verification

To verify the system identification results, a simulator was developed that used the coefficients from Table II and the motion predicted by the simulator was compared to the experimentally obtained motion data. Surge displacement results are presented in Figure 8 and surge velocity comparison results in Fig. 9.

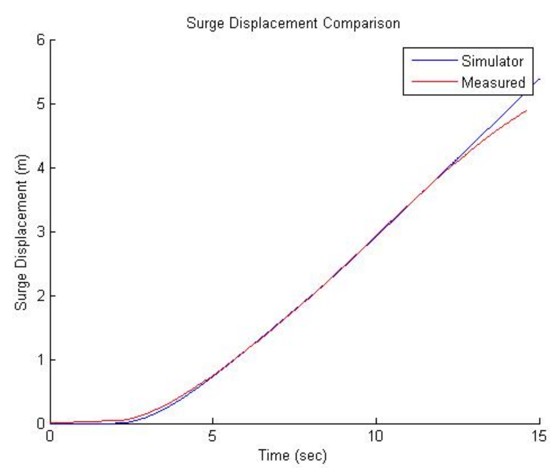

Fig. 8. Surge displacement comparison results

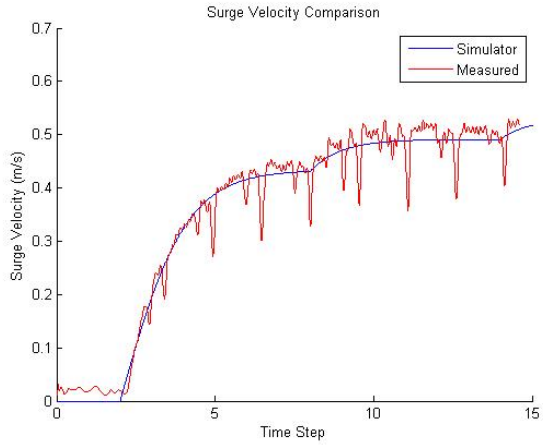

Fig. 9. Surge velocity comparison

The simulator's surge results, both in displacement and velocity, are very close to the actual measured experimental surge data. Simulated velocity results for the remaining degrees of freedom similarly match measured vehicle behavior and the graphical results are omitted.

The sway displacement results are similarly accurate, as can be seen from Fig. 10. A quantifiable delay exists on the physical system between specifying a command in software and this command reaching the vehicle (in part due to the vehicle tether). This delay is not currently accounted for in the simulator, but will be measured in future work. For the presented results, the simulator results are shifted to synchronize the simulated and measured initial vehicle response (the delay can be distinguished from vehicle dynamics by the graduate ramp-up of the vehicle displacement, which is accurately captured by the simulator).

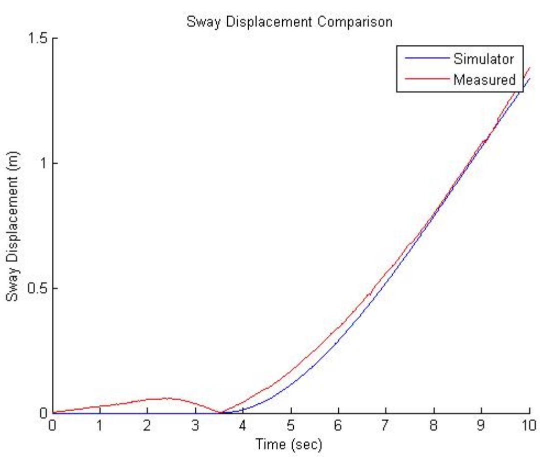

Fig. 10. Sway displacement comparison

Yaw and heave results are similarly accurate (see Fig. 11 and Fig. 12).

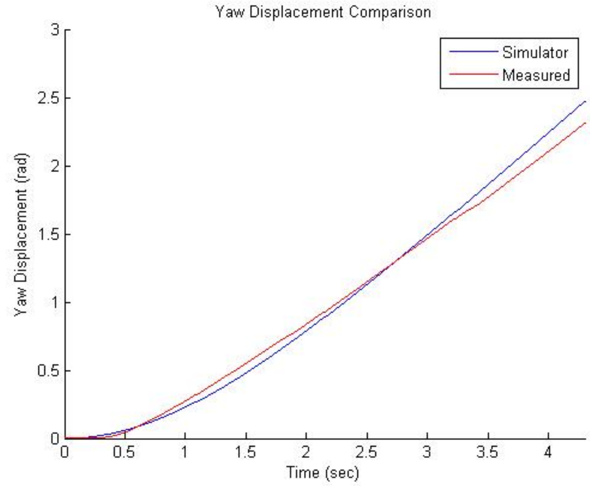

Fig. 11. Yaw displacement results

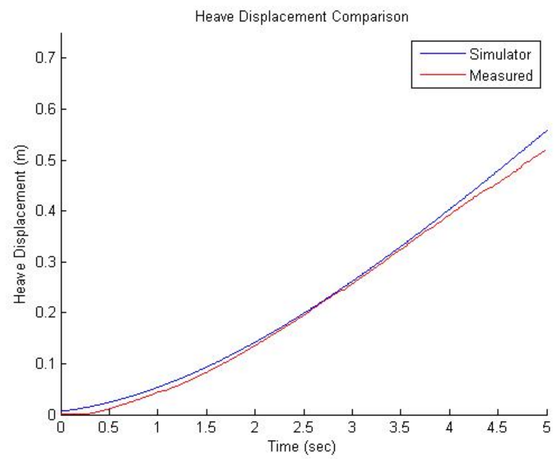

Fig. 12. Heave displacement results

VII. CONCLUSIONS AND FUTURE WORK

A six degree of freedom hydro dynamic model is developed for a UUV based on specific assumptions about its performance and operating envelope. The equations of motion for this model are manipulated to allow for sequential and accurate determination of all dynamic parameters. Based on these equations, an experiment is designed and a recursive least square estimator is implemented and verified using an existing model (with known parameters). The estimator is used to identify the surge, sway, heave, and yaw hydrodynamic parameters of the SeaBotix vLBV300 tethered AUV. The position and orientation of the vehicle is provided by an external motion capture system. The learned model is compared to the measured vehicle response and show excellent correlation. The experimental setup prevents the identification of the pitch and roll parameters. Furthermore, accurate calculation of the moments of inertia must be completed, but since these parameters only appear with the identified parameters, the overall response of the current model is not affected by this. The ability to recursively learn the hydrodynamic parameters has been demonstrated and these parameters can now be utilized by accurate control methods. Future work will include the use of an onboard INS to perform system identification and the development of said advanced control techniques.

REFERENCES

[1] T. Fossen, *Guidance and Control of Ocean Vehicles.* New York: John Wiley & Sons, 1994.

[2] J. J. E. Slotine and W. Li, “On-Line Parameter Estimation,” in *Applied Linear Control,* Englewood: Prentice-Hall, Inc, 1991, ch. 8, sec. 7, p. 358-381.

[3] [S. Thrun, W. Bulgard, and D. Fox, “Probabilistic Robotics”, MIT Press, Cambridge, MA, 2005.

[4] S. Sastry and M. Bodson, “Adaptive Control: Stability, Convergence, and Robustness”, Prentice Hall, Englewood Cliffs, New Jersey, 1989.

[5] Chen, H.H *et al*., “Identification of Hydrodynamic Properties for a Remotely Operated Vehicle Using Projective Mapping Method,” Institute of Undersea Technology and Asian Pacific ocean Research Center, Kaohsiung, Taiwan S.M Doherty, “Cross Body Thruster Control and Modeling of a Body of Revolution Autonomous Underwater Vehicle,” M.S. thesis, Dept. Mech. Eng, Naval Postgraduate School, Monterey, Ca, 2011.

[6] T. Prestero, “Verification of a Six-Degree of Freedom Simulation Model for the REMUS Autnonmous Underwater Vehicle,” M.S. thesis, Dept. Mech. Eng, Dept. Ocean Eng.,” MIT, Ma, 2001.

[7] K. Astrom and B. Wittenmark, “Real-Time Parameter Estimation,” in *Adaptive Control,* Addison-Wesley, 1994, ch 2, sec. 2, p 42-52.

[8] Eng, Y.H. *et al*. “Estimation of the Hydrodynamics Coefficient of an ROV using Free Decay Pendulum Motion,” *Engineering Letters,* vol. 16, no. 3, Aug 2008.

[9] F. Scarselli and A. Tsoi, “Universal Approximation Using Feedforward Neural Networks: A Survey of Some Existing Methods, and Some New Results,” *Neural Networks,* vol. 11, no. 1, p. 15-37, Jan. 1998.